A New Beamforming Process Based on the Phase Dispersion Analysis

Oscar Martínez-Graullera, David Romero-Laorden, Carlos J. Martín-Arguedas, Alberto Ibañez and Luis G. Ullate

CAEND (UPM-CSIC), C/ Serrano 144, Madrid 28006, Spain

Abstract. To improve the results of the Delay-And-Sum (DAS) beamformer a weighting factor based on a measurement of the phase dispersion of the signals in the image point under consideration has been proposed. With this objective, the spectral analysis of the phase dispersion is used here to obtain a new descriptor that can be easily computed and introduced as a ponderation factor in the beamforming process. Theoretical results show that, for a linear array of 32 elements operating in synthetic aperture technique with dynamic focussing in emission and reception (Total Focussing Method) the improvement can reach up to 24dB. In order to validate the theoretical hypothesis, experimental results obtained using a linear array of 64 elements (2,4MHz) and a CIRS 040GSE phantom also are presented.

Keywords: ultrasonic imaging, beamforming, SAFT
PACS: 87.63.dh, *43.60.-c, 87.85.Ng

INTRODUCTION

In synthetic aperture array ultrasonic imaging, the Full Matrix Array (FMA) process has been defined as the procedure that based on the independent operation of the transducer elements in an array, allows to acquire separately all the signals resulting from each combination of emission and reception elements. Thus, for a N array this process produces NxN signals that should be combined by a Total Focussing Method (TFM) to compose the image. Therefore, the TFM is a post-processing technique that uses the entire set of signals acquired by the system to focus at every point of the image. Its main advantage is to allow the simultaneous compensation of transmission and reception, offering the best angular lateral resolution possible at each image point [1]. However, its Signal to Noise Ratio (SNR) is limited by the low energy used in emission due to the small radiation area of the element. This often limits its practical use in field applications and precludes its development.

Although there are several research lines addressed to increase the level of energy in the medium based on code compression [2], our interest is focused on explore the capabilities of the beamforming process to increase the dynamic range. Beamforming is a signal processing technique used in ultrasonic sensor arrays for directional transmission and reception. In reception, the beamformer is a high performance spatial-temporal filter based on the Delay-And-Sum (DAS) technique that uses a FIR structure with multiple input signals.

In the last years there has been an increasing interest in the developing of Coherence Factor Methods. Generally speaking, coherence-based methods consist in weighting each point of the image according to the coherence estimated from the receive-aperture-domain data. As DAS, the coherence based beamformer is a non-adaptive and blind tool that uses the characteristic that element-signal-data from the mainlobe region are coherent, whereas those from the sidelobe region are incoherent. Hollman developed the coherence factor based on the energy analysis as a metric of image quality [3], showing that it can be used to increase drastically the dynamic range. Thus, it was incorporated into the DAS beamformer by Li and Li [4] and it has been proposed to be used combined with other adaptative beamforming techniques to improve medical imaging [5]. Recently, Camacho [6] has shown that phase evaluation can also be used as a coherence factor, and has proposed a statistical descriptor based on the variance of the phase distribution of the data used at each image point.

In this paper a new and alternative phase Coherence Descriptor based on the Fourier analysis of the phase distribution is presented.

SYNTHETIC APERTURE ULTRASONIC IMAGING BASED ON TFM

The set of complete signals obtained by a Full Matrix Capture procedure can be expressed as in-phase and quadrature components or can also be presented as modulus and phase components.

$$X_{e,r}(t) = I_{e,r}(t) + jQ_{e,r}(t) = \mathbf{X}_{e,r}(t)e^{j\phi_{e,r}(t)} \tag{1}$$

where $I_{e,r}(t)$ is the signal, obtained by the e-element emission and the r-element reception, and $Q_{e,r}(t)$ is the quadrature signal, obtained thorough the Hilbert Transform. Then $\mathbf{X}_{e,r}(t)$ is the modulus and $\phi_{e,r}(t)$ its corresponding signal phase. According to this nomenclature the DAS TFM image $A(x,z)$ can be computed as:

$$A(x,z) = \sqrt{\left(\sum_{e=1}^{N}\sum_{r=1}^{N} I_{e,r}(T(x,z))\right)^2 + \left(\sum_{e=1}^{N}\sum_{r=1}^{N} Q_{e,r}(T(x,z))\right)^2} \tag{2}$$

where $T(x,z)$ is a focussing delay for the point (x,z) that compensates emission and reception distances.

$$T(x,z) = \frac{\sqrt{(x-x_e)^2+z^2} + \sqrt{(x-x_r)^2+z^2}}{c} \tag{3}$$

where x_e and x_r are the coordinates of the elements e and r, and (x,z) is the space point under interest.

Image of Coherence Factor Map

Once the delays corresponding to each signal have been applied, at each image point a set of signal phases is obtained that is sorted to compose a phase distribution function by a sum of Kronecker deltas.

$$P(\phi) = \sum_{e=1}^{N}\left(\sum_{r=1}^{N}\delta[\phi - \phi_{e,r}(T(x,y))]\right) \tag{4}$$

where $\phi_{e,r}(T(x,z))$ is the phase of the signal emitted by e-element and collected by r-element compensated at (x,z). These values are distribute in the $[-\pi,\pi[$ interval and can be extended to form the periodic signal using a comb-function based on Dirac deltas:

$$\Phi(\phi) = \sum_{k=-\infty}^{\infty}\delta(\phi - k2\pi) * P(\phi) \tag{5}$$

In figure 1 it is shown how this function is composed for two image points of a simulated medium with a point reflector. A 64-element linear array has been simulated, and their 4096 signals have been computed with 30% of noise. Two points of the image have been selected: a point near to the reflector position (figure 1a), where the concentration of phases in a specific position is running; and in a location where there is no reflector point (figure 1b), where the phases are then uniformly distributed in the $[-\pi,\pi[$ range. The periodic extension of $P(\phi)$ is susceptible of being decomposed by Fourier Series into a sum of simple oscillating functions where each coefficient can be computed as:

$$c_n = \frac{1}{2\pi}\int_{-\pi}^{\pi}\Phi(\phi)e^{-j2\pi n f_o \phi}d\phi = \frac{1}{2\pi}\sum_{e=1}^{N}\left(\sum_{r=1}^{N} e^{-j2\pi n f_o \phi_{e,r}(T(x,z))}\right) \tag{6}$$

where, according to the signal period, $f_o = \frac{1}{2\pi}$. In figure 1 (c) it can be seen the values of c_n for the first 24 sinusoidal components of the Fourier series that correspond to the frequencies nf_o ($n = 0,...,24$). The signal $P(\phi)$ composed by a random distribution of phase spreads its energy over all the Fourier Coefficients which are low valued. However, when there is a concentration of phases it increases the presence of the sinusoidal components of period $\frac{1}{2\pi}$ than can be evaluated easily if $n = 1$ in equation 6. In order to normalise the result and obtain a more easy interpretation, our coherence factor at point (x,z) is defined as:

$$C_1(x,z) = (2\pi)c_1 = \sum_{e=1}^{N}\sum_{r=1}^{N} e^{-j\phi_{e,r}(T(x,z))} = \sum_{e=1}^{N}\sum_{r=1}^{N}(\cos(\phi_{e,r}(T(x,z))) - j\sin(\phi_{e,r}(T(x,z)))) \tag{7}$$

$$= \sum_{e=1}^{N}\sum_{r=1}^{N}\frac{I_{e,r}(T(x,z))}{\mathbf{X}_{e,r}(T(x,z))} - j\sum_{e=1}^{N}\sum_{r=1}^{N}\frac{Q_{e,r}(T(x,z))}{\mathbf{X}_{e,r}(T(x,z))} \tag{8}$$

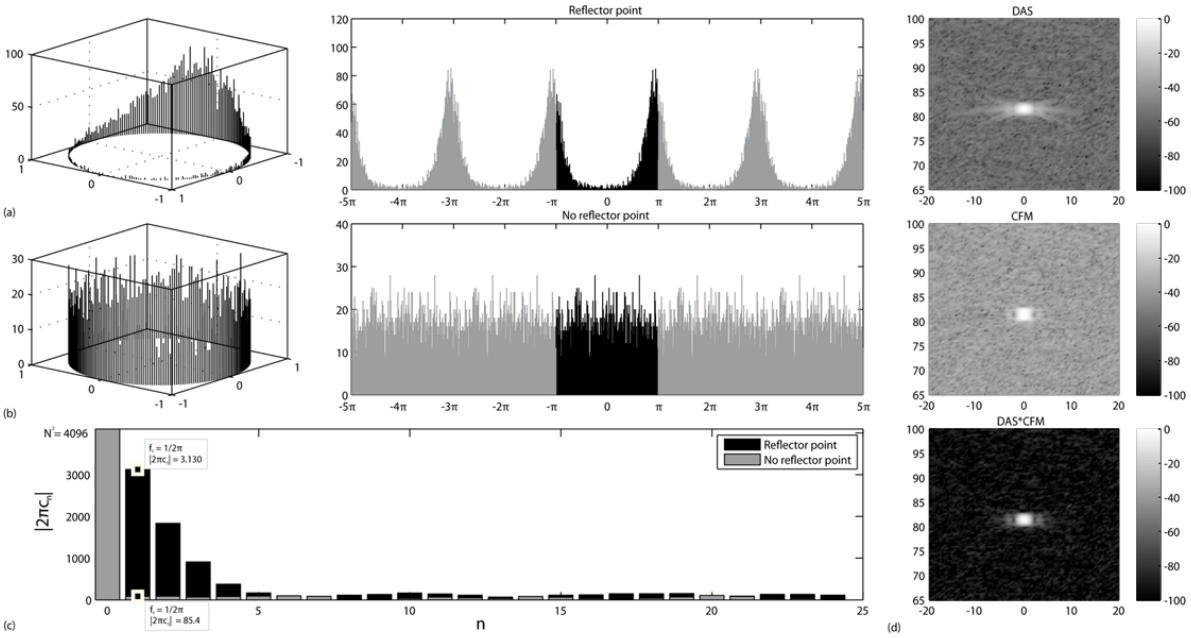

FIGURE 1. a) $P(\phi)$ in a point near to the reflector and its corresponding $\Phi(\phi)$; b) $P(\phi)$ in a no reflector point and its corresponding $\Phi(\phi)$ function; c) The first 24 coefficients of Fourier series for both points, the component $f_\phi = \frac{1}{2\pi}$ has been remarked; d) The images of the reflector point for DAS, CFM and DASxCFM

The maximum value of this function is achieved when all phase components are concentrated and is NxN (4096 in this case), which is the total number of signals involved in the process. In figure 1 the coherence has been measured at the reflector point that is contributed by 3130 signals (a), and in the point where there is no reflector the coherence is reduced to be composed by 85 signals (b).

The complete image Coherence Factor Map (CFM) can be expressed then by:

$$H(x,z) = |C_1(x,z)| \tag{9}$$

and the new image equation as:

$$I(x,z) = A(x,z)H(x,z) \tag{10}$$

In figure 1 (d) the corresponding DAS, CFM and DASxCFM images are represented with a dynamic range of 100dB (from top to bottom). The DAS presents a dynamic range around 49dB. The CFM dynamic range has a mean value of 30dB, and in its image there is no a significant sidelobe distribution. Both aspects are introduced in our final image, reducing sidelobes and improving the global dynamic range up to 80dB.

EXPERIMENTAL RESULTS

As experimental procedure a Phantom (CIRS, 040GSE) was examined using a 2.6MHz phased array transducer of 64 elements. Using a FMA process, the 4096 array signals were obtained and the TFM image was composed for the DAS algorithm, the CFM, and the combination of DAS and CFM. The selected region is composed by four wires and the cyst. The results are presented in figure 2, where dynamic range has been limited to 70dB. Furthermore two in-deep profiles are presented from DAS, CFM and DASxCFM images: one corresponding to the cyst and one wire ($x = -21$), and the other to the position of the three wires ($x = -10$). The dynamic range in the DAS image is around 33dB. The CFM image shows the same elements with a dynamic range of at least 24dB, in this case wires present levels near to 0dB and the cyst is at -10dB. In the resultant image DASxCFM, it means that dynamic range has increased 24dB in the wires and 10dB in the cyst, providing in general a dynamic range near of 55dB. Differences with theoretical result can be caused by errors introduced in the digitalisation process and interferences due to structural elements in the medium (other cyst and wires) that reduce the contribution of the elements.

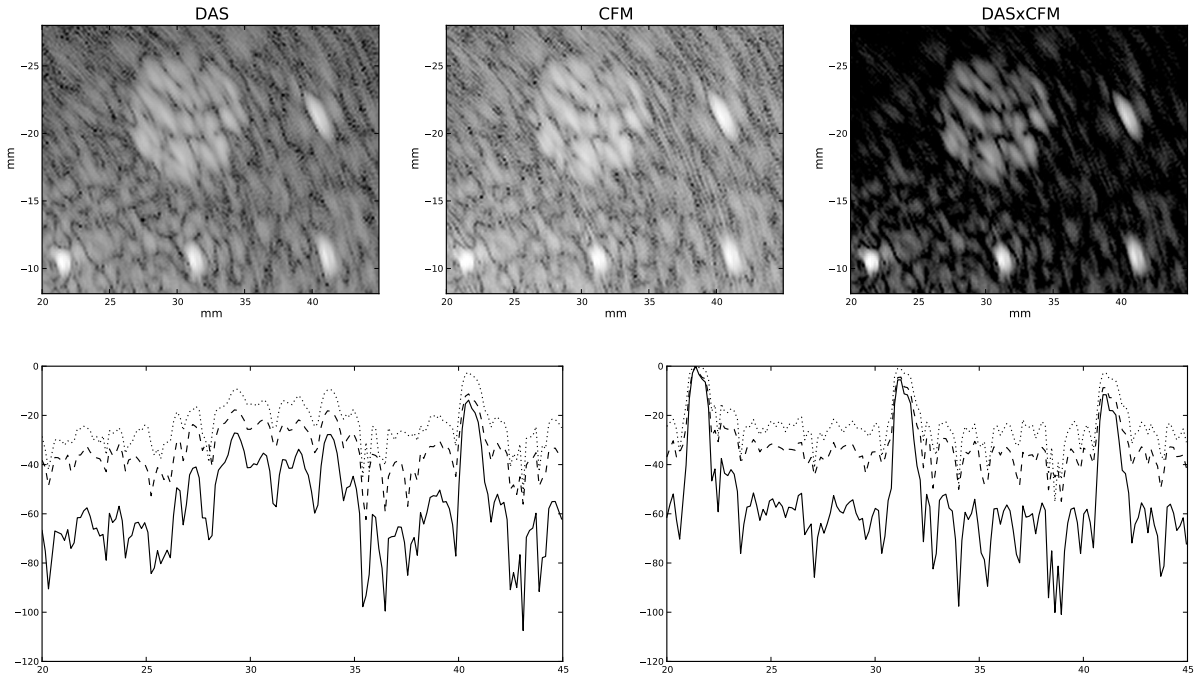

FIGURE 2. Top: DAS, CFM and DASxCFM images of a cyts and four wires locates at ($x = -8 : -40$mm, $z = 20 : 45$), dynamic range in the images has been limited to -70dB. Bottom: in deep profiles for DAS (dashed line), CFM (dotted line), and DASxCFM (continuous line), in $x = -21$ (left) and $x = -10$ (right).

CONCLUSIONS

With the objective of increasing the dynamic range in SAFT image a new descriptor for the Coherence Factor Method based on Fourier analysis of the phase distribution has been developed. A theoretical study has been presented and its results have been validated by simulated and experimental data. The implementation of this new Coherence Factor is simple and paradoxically it can be obtained without explicit computation of the phase. Furthermore, it can be easily integrated in a traditional beamformer. The increment in the dynamic range achieved by the Coherence Factor Map is limited to the number of signals involved but is independent of the amplitude of the echo response. Because of that it is robust against attenuation and noise.

ACKNOWLEDGMENTS

This work has been supported by the Spanish Ministry of Science and Innovation under the project DPI2010-19376

REFERENCES

1. C. Holmes, B.W. Drinkwater and P.D. Wilcox, *Ultrasonics* **48**, 636–642 (2008).
2. R.Y. Chiao and X. Hao, *Trans. on UFFC* **52(2)**, 160–170 (2005).
3. K. W. Hollman, K. W. Rigby and M. O'Donnell, in *Proc. of the IEEE Ultrasonics Symposium*, pp. 1257–1260 (1999).
4. P. Li and M. Li, *Trans. on UFFC* **50(2)**, 128–141 (2003).
5. C.C. Nilsen and S. Holm, *Trans. on UFFC* **57(6)**, 1329–1346 (2010).
6. J. Camacho, M. Parrilla and C. Fritsch, *Trans. on UFFC* **56(5)**, 958–974 (2009).